ELSEVIER

Biophysical Chemistry 67 (1997) 85–96

Biophysical Chemistry

Electrostatic contribution to the bending of DNA

Andrei Sivolob *, Sergei N. Khrapunov

Department of General and Molecular Genetics, National Shevchenko University, 252601 Kiev, Ukraine

Received 30 August 1996; revised 6 January 1997; accepted 29 January 1997

Abstract

A model is derived that accounts for the short-range electrostatic contribution to the bending of DNA molecule in solution and in complexes with proteins in terms of the non-linear Poisson–Boltzmann equation. We defined that the short-range electrostatic interactions depend on the changes of the polyion surface charge density under deformation, while the long-range interactions depend on the bending-induced changes in distances between each two points along the polyion axis. After an appropriate simplification of the Poisson–Boltzmann equation, the short-range term is calculated separately giving the lower limit for the electrostatic contribution to the DNA persistence length. The result is compared with the theoretical approaches developed earlier [M. Fixman, J. Chem. Phys. 76 (1982) 6346; M. Le Bret, J. Chem. Phys. 76 (1982) 6243] and with the experimental data. The conclusion is made that the results of Fixman–Le Bret, which took into account both types of the electrostatic interactions for a uniformly bent polyion, give the upper limit for the electrostatic persistence length at low ionic strength, and the actual behavior of the DNA persistence length lies between two theoretical limits. Only the short-range term is significant at moderate-to-high ionic strength where our results coincide with the predictions of Fixman–Le Bret. The bending of DNA on the protein surface that is accompanied by an asymmetric neutralization of the DNA charge is also analyzed. In this case, the electrostatic bending energy gives a significant favorite contribution to the total bending energy of DNA. Important implications to the mechanisms of DNA-protein interactions, particularly in the nucleosome particle, are discussed. © 1997 Elsevier Science B.V.

Keywords: DNA electrostatics; Poisson–Boltzmann equation; DNA bending; DNA-protein interactions; Nucleosome structure

1. Introduction

An understanding of the mechanisms of DNA bending is very essential for the comprehensive consideration of different phenomena of DNA packaging and functioning. DNA is tightly bent in a phage head and in both prokaryotic and eukaryotic chromosomes. In the nucleosome, the elementary unit of eukaryotic chromatin, DNA wraps around a protein core as a superhelix with a radius of 4.3 nm [1,2]. The latter is very important, for example, in nucleosome positioning with respect to the DNA sequence [2–4]. The binding to DNA of different regulatory proteins is accompanied by a DNA bending, and this fact may be important for protein–DNA recognition [3,5–8]. One of the substantial physical features of DNA is its high axial charge density and this fact may essentially influence DNA bendability. Several experimental studies of the dependence of DNA flexibility on ionic strength are described [9–13] (see also reviews [14,15]). It seems likely that the most exact results have been obtained for short DNA

* Corresponding author.

PII S0301-4622(97)00022-7

fragments, for which the excluded volume effects are negligible. Analysis of the rotational relaxation times of the transient electric birefringence of short DNA fragments [9] indicates that the persistence length (the measure of the bending rigidity of a worm-like polymer [16]) does not depend on the salt concentration above 1 mM NaCl or 0.1 mM $MgCl_2$, and considerably increases for lower ionic strength values. Likewise, the ring-closure measurements [12] demonstrate that over a range of NaCl concentration from 0 to 162 mM (in 1 mM $MgCl_2$), there is no significant reduction in the DNA persistence length.

There are two questions: (1) what is the physical basis for such behavior of DNA flexibility in solution, and (2) what is the electrostatic contribution to DNA bending in protein–DNA complexes. Here, we address both of these problems. The electrostatic contribution to the persistence length of polyelectrolytes has been calculated by several authors [17–24]. Probably the most prominent theoretical approach has been done by Fixman [22] and Le Bret [23] on the basis of the full (non-linear) Poisson–Boltzmann (PB) equation for a uniformly bent cylinder. As discussed below, the results of these calculations, which are in a qualitative agreement with the experiment, give an upper limit for the polyelectrolyte contribution to the DNA flexibility. In the present work, we suggest a more simple model, which is also based on the non-linear PB equation. This model allows us to give a more clear description of the problem considering two electrostatic terms: the short-range electrostatic interactions which depend on the changes of the polyion surface charge density under deformation, and the long-range interactions which depend on the bending-induced changes in distances between each two points along the polyion axis. Taking into account only the first term, we obtain a lower limit for the electrostatic persistence length, estimate the relation between two types of electrostatic interactions at different salt concentrations and evaluate the electrostatic contribution to DNA bending under asymmetric phosphate neutralization by proteins.

2. General model

It is a consensus that up to an ionic strength of about 1 M the Poisson–Boltzmann (PB) equation for continuously charged impermeable cylinder gives, with a reasonable accuracy, reliable data for the electrostatic potential and the charge density distribution around the polyion [25]. So, we model the DNA molecule as a cylinder of radius $a = 1$ nm with a given surface charge density σ_0 (in units of elementary charge e). The parameter which characterizes the polyion axial charge density is designated as

$$\xi = B/b \tag{1}$$

where $B = e^2/Dk_BT$ is the Bjerrum length (with D is the dielectric constant, k_B is the Boltzmann constant and T is the absolute temperature), b (for DNA $b = 0.17$ nm) is the length of a cylinder segment containing a unit charge. For aqueous solution at 25°C, $B = 0.714$ nm and then for DNA $\xi = 4.2$. The relation between ξ and σ_0 is

$$\xi = 2\pi aB\sigma_0 \tag{2}$$

The general form of the PB equation, which relates the electrostatic potential Ψ at any point outside the cylinder to mobile ion charge density at that point is:

$$\nabla^2 f = \kappa^2 \sinh(f) \tag{3}$$

where $f = e\Psi/k_BT$ is the reduced potential, κ is the Debye–Hückel screening parameter, operator ∇^2 is the Laplacian. So, the mobile ion charge density is $2en_0\sinh(f) = en_0[\exp(f) - \exp(-f)]$ (for simplicity both counterions and coions are taken to be univalent), where n_0 is the density of mobile ions at infinity from polyion surface. The parameter κ relates to this value as:

$$\kappa^2 = 8\pi Bn_0 \tag{4}$$

or, in aqueous solution at 25°C, $\kappa^2 = 10.824C\ \mathrm{nm}^{-2}$, where C is the molar concentration of 1:1 salt. In particular, for the potential f_0 of a straight cylinder, when the Laplacian depends only on the distance r from the polyion axis, the PB Eq. (3) has the form

$$\frac{1}{\kappa r}\frac{\mathrm{d}f_0}{\mathrm{d}(\kappa r)} + \frac{\mathrm{d}^2 f_0}{\mathrm{d}(\kappa r)^2} = \sinh(f_0) \tag{5}$$

with two boundary conditions:

$$(\mathrm{d}f_0/\mathrm{d}(\kappa r))_\infty = 0 \tag{6a}$$

$$(\mathrm{d}f_0/\mathrm{d}(\kappa r))_a = -2\xi/\kappa a \tag{6b}$$

Let us consider now an infinitely long cylinder, which is uniformly bent with a curvature radius R. Two factors change under such deformation. Firstly, the charge density on the polyion surface becomes non-uniform, i.e., an angular dependence should be included to the Laplacian and also the boundary conditions should be changed. These changes in the electrostatics of the system can be defined as changes of short-range (with respect to distances along the polyion axis) electrostatic interactions. Secondly, distances between each two points along the axis decrease under deformation, i.e., long-range electrostatic interactions also change. These changes should be taken into account by an appropriate choice of the coordinate system, for which the corresponding Laplacian should be written. Let us note that the long-range interactions in our definition are not related in any fashion to the excluded volume effects, which depend on the interactions between very far, uncorrelated regions of the polymer coil.

Fig. 1 illustrates the curvilinear orthogonal coordinate system, which should be used to solve the PB equation for bent cylinder [22]. One can see that three coordinates (r,φ,s) determine the position of a given point. We restrict the solution to regions distant from the ends of the cylinder, i.e., we assume that the potential is independent of s. Also, we assume that the cross sections of the cylinder remain circular under deformations, and any element of cylinder surface retains exactly the charge that it had before deformation. Inspection of Fig. 1 indicates that the axial size of the surface element, which contains one elementary charge, changes under deformation from b to bh_a, where $h_a = h(a,\varphi)$ and

$$h(r,\varphi) = R(r,\varphi)/R = 1 + (r/R)\cos(\varphi) \qquad (7)$$

Consequently, taking into account Eq. (2), the surface charge density varies with R and φ as

$$\sigma = \sigma_0/h_a = \xi/2\pi aBh_a \qquad (8)$$

It means that the axial charge density ξ does not change after bending deformation [22,24,26]. Finally, we suppose for simplicity that the ratio of dielectric constants inside and outside the cylinder ϵ equals to zero (estimate that is close to any plausible estimate of this ratio [22]).

With the simplifications mentioned above, the PB equation can be written for the potential f of a bent cylinder [22]

$$\frac{1}{\kappa r}\frac{\partial f}{\partial(\kappa r)} + \frac{\partial^2 f}{\partial(\kappa r)^2} + \frac{1}{(\kappa r)^2}\frac{\partial^2 f}{\partial\varphi^2} + \frac{\partial \ln(h)}{\partial(\kappa r)}\frac{\partial f}{\partial(\kappa r)} + \frac{1}{(\kappa r)^2}\frac{\partial \ln(h)}{\partial\varphi}\frac{\partial f}{\partial\varphi} = \sinh(f) \qquad (9)$$

where $h \equiv h(r,\varphi)$ according to Eq. (7), with the boundary condition on the polyion surface (see Eqs. (6b) and (8)).

$$(\partial f/\partial(\kappa r))_a = -4\pi B\sigma/\kappa = -2\xi/h_a\kappa a \qquad (10)$$

After expansion of Eq. (9) in inverse powers of R and using a Fourier decomposition for the potential, Fixman has solved this equation numerically and used the coefficient of R^{-2} for an estimation of the electrostatic contribution to the persistence length [22]. However, a uniform bending (excepting the special case of intrinsically bent DNA molecules) is impossible in solution where the direction of curvature at any point along the chain is random. At the same average curvature in the chain, the average distance between two points along the polyion axis in the case of random deformations is obviously higher than for the uniform bending. So, the uniform bending model and the application of Eq. (9) would lead to an overestimate of the electrostatic persistence length.

Looking now at the Laplacian in Eq. (9), one can see that the three first terms are the usual Laplacian in cylindrical coordinates, and the last two terms are the correction for a curvature of the coordinate sys-

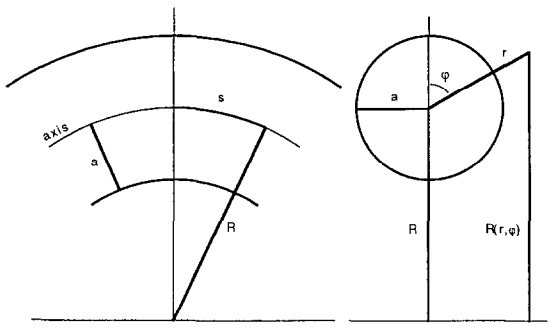

Fig. 1. The curvilinear coordinate system in the plane of the bent polyion cylinder (left) and in the perpendicular plane (right). The cylinder radius a, the curvature radius R and three coordinates r,φ,s are shown.

tem. That is, the last two terms take into account the long-range electrostatic interactions. Our general suggestion is that these terms can be omitted to estimate only the short-range electrostatic interactions under polyion bending and then to compare the results with the Fixman's data. Thus, we can write the PB equation for the potential of a uniformly bent cylinder in the form:

$$\frac{1}{\kappa r}\frac{\partial f}{\partial(\kappa r)} + \frac{\partial^2 f}{\partial(\kappa r)^2} + \frac{1}{(\kappa r)^2}\frac{\partial^2 f}{\partial \varphi^2} = \sinh(f) \tag{11}$$

with Eq. (10) as the boundary condition. Thus, we use the PB equation for a straight cylinder with the boundary conditions for a deformed DNA rod. In other words, we take into account a change in the surface charge density under deformation neglecting the change in the overall geometry of the system, which is given by the omitted terms in the Laplacian. The comparison between the results obtained with rigorous and simplified Laplacian will then show a relation between the short- and long-range electrostatic interactions. Certainly, this approach may be valid only in the limit of small deviations from rodlike behavior, i.e., large curvature radius R (the same assumption has been made by Fixman and Le Bret [22,23]). Eq. (11) will be examined below, and its relation to Eq. (9) will be discussed. The fact that Eqs. (9) and (11) give the same results at given conditions (see below) supports the validity of the approximation used in Eq. (11).

The model of a uniformly bent cylinder can be applied to study an important case of DNA bending under its interaction with proteins. Fig. 2 specifies our simple model of a protein–DNA complex. DNA (as a cylinder) bends on the protein surface, which covers a part θ (with respect to the φ angle) of the DNA surface. We assume, to a first-order approximation, that the DNA charges are completely neutralized in the area of protein–DNA contact (the degree of neutralization equals to θ), and that distortions of the electrostatic field near the protein surface are negligible. So, Eq. (11) would be applied to this case with Eq. (10) as the boundary condition within the range of φ angle between 0 and $\pi(1-\theta)$. For φ angle between $\pi(1-\theta)$ and π, we put that the surface charge density and the electrostatic potential

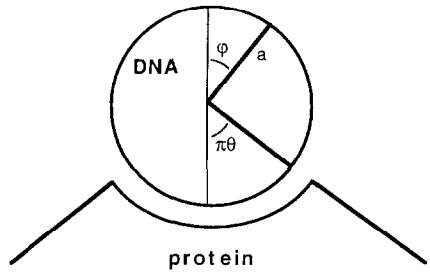

Fig. 2. The model of DNA bending on the protein surface in a plane perpendicular to the axis of bent DNA (as in the right side of Fig. 1). DNA charge is completely neutralized within the angle $\pi\theta$.

equals to zero. The real electrostatics of DNA-protein complex may be of course much more complicated. Our simple model is an approximation to study, in a semi quantitative manner, the role of asymmetrical neutralization of DNA phosphates.

3. Electrostatic free energy and solution of PB equation

3.1. Uniform bending

We consider here the uniform bending model specified in previous section (see Figs. 1 and 2). The electrostatic free energy of polyion is the work required to raise its surface charge density from zero to its final value σ. So, taking into account Eqs. (2) and (8) and the fact that the plane of curvature is a plane of mirror symmetry (Fig. 1, right), the electrostatic free energy G_{el} in $k_B T$ units per one elementary charge of the polyion (one phosphate residue) can be written as:

$$G_{el} = (\pi\xi)^{-1}\int_0^{\pi}\int_0^{\xi} f(a)\,\mathrm{d}\xi\,\mathrm{d}\varphi \tag{12}$$

where $f(a)$ is the potential on the polyion surface. We will use this equation everywhere below. It should be noted, however, that the equivalent formulation exists for the electrostatic free energy, which includes the integration of functions of the potential over the volume of the ion atmosphere around the polyion [27]. This formulation, which allows to estimate different contributions that have the clear physical meaning, is described briefly in Appendix A. It

is shown that the main contribution into the electrostatic free energy is the mixing entropy of mobile ions assembled around DNA.

The solution of Eq. (11) is now required. We assume that the potential f is the sum of two terms

$$f = f_0 + f_b \tag{13}$$

where f_0 is the potential of the straight cylinder determined by Eq. (5), f_b is the change of the potential under deformation, and, for high values of R, $|f_b| \ll |f_0|$. Then, from Eqs. (5), (11) and (13), we obtain the differential equation for f_b:

$$\frac{1}{\kappa r}\frac{\partial f_b}{\partial(\kappa r)} + \frac{\partial^2 f_b}{\partial(\kappa r)^2} + \frac{1}{(\kappa r)^2}\frac{\partial^2 f_b}{\partial \varphi^2} = f_b \cosh(f_0) \tag{14}$$

The expansion of the right side of Eq. (10) in inverse powers of κR gives the boundary condition for f_b on the polyion surface (see also Eqs. (6b), (7) and (13)):

$$\left(\partial f_b/\partial(\kappa r)\right)_a = -\frac{\xi\kappa a}{(\kappa R)^2} + \frac{2\xi}{\kappa R}\cos(\varphi) - \frac{\xi\kappa a}{(\kappa R)^2}\cos(2\varphi) \tag{15}$$

where only terms with no more then second powers of $1/R$ are included.

If we put that the potential f_b can be written as a product of two terms $f_b = f_r f_\varphi$ so that f_r depends only on κr and f_φ depends only on φ, then the variables in Eq. (14) can be divided and we obtain two differential equations for two variables κr and φ:

$$\frac{\kappa r}{f_r}\frac{\mathrm{d}f_r}{\mathrm{d}(\kappa r)} + \frac{(\kappa r)^2}{f_r}\frac{\mathrm{d}^2 f_r}{\mathrm{d}(\kappa r)^2} - (\kappa r)^2 \cosh(f_0) = n^2 \tag{16a}$$

$$\frac{1}{f_\varphi}\frac{\mathrm{d}^2 f_\varphi}{\mathrm{d}\varphi^2} = -n^2 \tag{16b}$$

where n^2 is the dividing constant.

Let us consider firstly Eq. (16b). The boundary conditions for it are obvious from the reasons of symmetry (Fig. 1):

$$\left(\mathrm{d}f_\varphi/\mathrm{d}\varphi\right)_0 = \left(\mathrm{d}f_\varphi/\mathrm{d}\varphi\right)_\pi = 0 \tag{17}$$

and the analytical solution can be easily obtained as a sum of special solutions, which have the form of the terms of a Fourier series:

$$f_\varphi = \cos(n\varphi),\ n = 0,1,2,\cdots \tag{18}$$

Comparison of these solutions with the boundary condition (Eq. (15)) implies that the term f_r should be expanded also in inverse powers of kR, and the following equations with the corresponding boundary conditions can be generated from Eq. (16a) for different values of n from 0 to 2:

$$\frac{1}{\kappa r}\frac{\mathrm{d}f_{20}}{\mathrm{d}(\kappa r)} + \frac{\mathrm{d}^2 f_{20}}{\mathrm{d}(\kappa r)^2} = f_{20}\cosh(f_0)$$

$$\left(\mathrm{d}f_{20}/d(\kappa r)\right)_a = -\xi\kappa a \tag{19a}$$

$$\frac{1}{\kappa r}\frac{\mathrm{d}f_{11}}{\mathrm{d}(\kappa r)} + \frac{\mathrm{d}^2 f_{11}}{\mathrm{d}(\kappa r)^2} = f_{11}\cosh(f_0) + \frac{f_{11}}{(\kappa r)^2}$$

$$\left(\mathrm{d}f_{11}/\mathrm{d}(\kappa r)\right)_a = 2\xi \tag{19b}$$

$$\frac{1}{\kappa r}\frac{\mathrm{d}f_{22}}{\mathrm{d}(\kappa r)} + \frac{\mathrm{d}^2 f_{22}}{\mathrm{d}(\kappa r)^2} = f_{22}\cosh(f_0) + \frac{4f_{22}}{(\kappa r)^2}$$

$$\left(\mathrm{d}f_{22}/\mathrm{d}(\kappa r)\right)_a = -\xi\kappa a \tag{19c}$$

That is, we finally obtain for f_b:

$$f_b = f_{20}/(\kappa R)^2 + f_{11}\cos(\varphi)/(\kappa R) + f_{22}\cos(2\varphi)/(\kappa R)^2 \tag{20}$$

Eqs. (19a), (19b) and (19c) can be solved numerically provided that the numerical solution for f_0 has been obtained from Eq. (5). To solve Eqs. (5), (19a), (19b) and (19c) for f_{ij} ($f_{00} \equiv f_0$) we apply a usual fourth-order Runge–Kutta integration routine. The integration is initiated at a large value of κr (the result is not sensitive to this value provided that the initial $\kappa r > 6$), where the first derivative of the potential $\mathrm{d}f_{ij}/\mathrm{d}kr = 0$ (The condition in Eq. (6a) has to be taken for all equations) and f_{ij} has a small value, which is considered as unknown parameter to be adjusted by iteration until the solution fulfills the boundary condition on the polyion surface. The numerical method applied is standard and has been used frequently. It should be noted only that Eq. (5) is solved on a grid with half the spacing used for Eqs. (19a), (19b) and (19c) (as it is required by Runge–Kutta routine).

The calculations are performed for different values of ξ from 0 to 4.2 (at a given value of the ionic strength). As a result, we obtain the potentials on the polyion surface, and the electrostatic free energy can be determined now according to Eq. (12), where the integration over ξ has to be done numerically while the angular integration is analytical. The upper limit of the angular integral is π for the naked cylinder, or $\pi(1-\theta)$ for the model of a protein–DNA complex specified in Fig. 2.

We designate

$$I_{ij} = \int_0^{\xi} f_{ij}(a)\,\mathrm{d}\xi \tag{21}$$

Substitution of Eqs. (20) and (21) into Eq. (12) gives a general form for the electrostatic free energy of DNA bending (change of the free energy with respect to the straight cylinder) in $k_B T$ units per one phosphate:

$$\begin{aligned}\Delta G_{el}(\theta) = (\xi\pi)^{-1}(\kappa R)^{-2}\{&\pi(1-\theta)I_{20} \\ &+ \kappa R I_{11}\sin(\pi(1-\theta)) \\ &+ (1/2)I_{22}\sin(2\pi(1-\theta))\}\end{aligned} \tag{22}$$

which can be applied to estimate the electrostatic contribution to the bending free energy of DNA in protein–DNA complexes with a given value of θ. It should be noted that the gain in the total free energy due to electrostatic interactions between DNA and protein, which is beyond the scope of the present work, is not included into Eq. (22).

In the special case of $\theta = 0$ (naked cylinder), we obtain

$$\Delta G_{el} = \xi^{-1}(\kappa R)^{-2} I_{20} \tag{23}$$

that is, only potential f_{20} is required to estimate the electrostatic contribution to the persistence length. The total free energy of bending (in $k_B T$ units per one phosphate) is given by [16]:

$$\Delta G_{bend} = b(p_0 + p_{el})/2R^2 \tag{24}$$

where p_0 and p_{el} are the non-electrostatic and electrostatic contributions to the persistence length, respectively. Comparison of Eqs. (23) and (24) (taking into account Eq. (1)) gives:

$$p_{el} = 2I_{20}/B\kappa^2 \tag{25}$$

3.2. Random bending fluctuations

In this section we describe an equivalent approach to calculation of the electrostatic persistence length, which takes into account the short-range electrostatic interactions of a non-uniformly bent cylinder. The standard representation of DNA as a worm-like coil treats the polymer as a continuously curving chain for which the direction of curvature at any point along the chain is random [16]. Hence, a mean-square curvature, and, respectively (see Eqs. (7) and (8)), a root-mean-square addition to the surface charge density appear in the polyion. To take into account the short-range electrostatic interactions only, the PB equation should be written as for a straight cylinder with the changed charge density. So, we have the PB equation:

$$\frac{1}{\kappa r}\frac{\mathrm{d}f}{\mathrm{d}(\kappa r)} + \frac{\mathrm{d}^2 f}{\mathrm{d}(\kappa r)^2} = \sinh(f) \tag{26}$$

and the boundary condition on the polyion surface:

$$(\mathrm{d}f/\mathrm{d}(\kappa r))_a = -4\pi B\langle\sigma\rangle/\kappa \tag{27}$$

where $\langle\sigma\rangle$ is the angular average charge density over φ. After expansion of σ in Eq. (8) in inverse powers of kR (as in Eq. (15)) and integration over φ from 0 to π, we obtain:

$$\langle\sigma\rangle = (2\pi aB)^{-1}\xi\left[1 + (1/2)(\kappa a)^2/(\kappa R)^2\right] \tag{28}$$

This relation implies that the potential f can be represented as

$$f = f_0 + f'/(\kappa R)^2 \tag{29}$$

and, if $f'/(\kappa R)^2 \ll f_0$, from Eqs. (5), (6b), (26)–(29) we obtain the equation for f' and the boundary condition:

$$\begin{aligned}&\frac{1}{\kappa r}\frac{\mathrm{d}f'}{\mathrm{d}(\kappa r)} + \frac{\mathrm{d}^2 f'}{\mathrm{d}(\kappa r)^2} = f'\cosh(f_0) \\ &(\mathrm{d}f'/\mathrm{d}(\kappa r))_a = -\xi\kappa a\end{aligned} \tag{30}$$

Eq. (30) is equivalent to Eq. (19a) for f_{20} which is sufficient to estimate the electrostatic contribution to the persistence length due to the short-range electrostatic interactions (Eq. (25)). Thus, as it has been

expected, this estimation does not depend on the choice between the models of a uniform bend and random bending fluctuations.

4. Electrostatic contribution to DNA persistence length

Our model accounts for the electrostatic contribution to the polyion persistence length in terms of the short-range electrostatic interactions that depend only on the changes of polyion surface charge density under deformation. As it can be seen from Section 3.2, the electrostatic contribution to the persistence length using only short-range electrostatic interactions is independent of the assumed bending model (uniform bending or random bending fluctuations). Thus, our approach allows us to calculate a lower limit for the electrostatic persistence length. From the other hand, the approaches derived by Fixman [22] and Le Bret [23], which are based on the uniform bending model, take into account both the short- and the long-range electrostatic interactions that depend on changes in distances between each two points along the polyion axis. It is clear that, since non-uniform random bending fluctuations in different directions occur in solution, the long-range interactions are somewhat overestimated by these models, which, consequently, give the upper limit for the electrostatic persistence length.

The results of our calculations are shown in Fig. 3 in comparison with the data of Fixman [22] (which practically coincide with the results of Le Bret, small discrepancy takes place only for 0.1 mM salt [23]). In other words, Fig. 3 presents the two theoretical limits for the electrostatic contribution to the DNA persistence length at different ionic strength values (for 1:1 salt). Some experimental results are also presented in Fig. 3. To obtain an approximate coincidence between theoretical predictions for the electrostatic contribution p_{el} into persistence length and the experimental results obtained at high ionic strength, we subtract 35 nm (assumed to be the value of p_0 in Eq. (24)) from all experimental total persistence length values. A difference between the results of transient electric birefringence study of short DNA fragments [9], and light scattering [10] and flow birefringence [11] investigations of long DNA

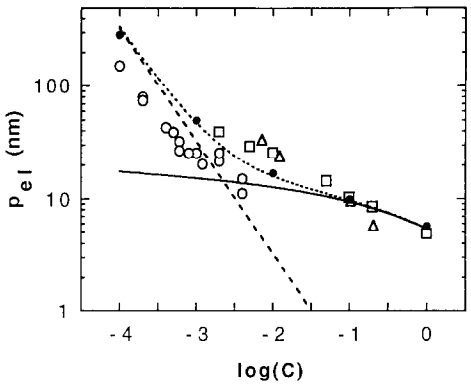

Fig. 3. The electrostatic contribution to the persistence length of DNA as a function of molar 1:1 salt concentration (smooth curve). The filled circles represent the result of calculations performed by Fixman (for 1:1 salt and $\varepsilon = 0$) [22]. The dashed line represents the salt-dependence of p_{cond} according to Eq. (32), the dotted line is the sum of the smooth and dashed curves. The experimental data of Hagerman [9] (open circles), Kam et al. [10] (triangles), and Cairney and Harrington [11] (rectangles, the set of data with nucleotide optical anizotropy factor -12.711 is taken) are also presented. From all original experimental points the constant value 35 nm (assumed as p_0 in Eq. (24)) was subtracted to facilitate comparison with the theoretical predictions.

molecules has not been resolved. This difference may, in part, be due to electrostatic end effects in short chains [28]. On the other hand, a gradual decrease in the persistence length with increasing salt concentration [10,11] is most likely due to the problem with correction for excluded volume [15]. Note, that the value obtained by Kam et al. [10] in 1 M Na^+ (total persistence length is 30.3 nm) is not presented in Fig. 3. The conclusion that the persistence length does not depend on the salt concentration above 1 mM NaCl or 0.1 mM $MgCl_2$ [9] has been supported by the ring-closure measurements [12] and the recent observation that the DNA helix is likely to possess substantial rigidity in the absence of phosphate interactions [29].

According to Fixman [22] and Le Bret [23], electrostatic persistence length decreases by a factor about 3 with the increase of ionic strength from 1 to 10 mM for a 1:1 salt (and by a factor about 2 for a 2:1 salt). According to our model, electrostatic persistence length decreases only slightly in this range of 1:1 salt concentrations. The actual dependence of the persistence length on the ionic strength in low-salt region [9] lies between two theoretical limits in Fig.

3, and the results obtained in moderate-to high ionic strength regions [10,11] are in good agreement with the theoretical predictions.

It is not surprising that the long-range interactions essentially contribute to the electrostatic persistence length only at very low ionic strength: two models give practically coinciding results for the ionic strength above 10 mM (Fig. 3). It has been shown in earlier calculations [17,18] that the electrostatic persistence length in Debye–Hückel approximation is given by:

$$p_{DH} = \xi^2/4B\kappa^2 \quad (31)$$

Since a linear array of point charges was considered [17,18], Eq. (31) estimates only the long-range electrostatic interactions and this estimation is rather accurate in the low-salt limit. A modification of this equation for highly charged polyelectrolyte according to the condensation theory [20] gives [22]:

$$p_{cond} = 1/4B\kappa^2 \quad (32)$$

or, in aqueous solution at 25°C, $p_{cond} = 0.032\ C^{-1}$ nm. The dashed line in Fig. 3 is calculated according to this relation. It is interesting that the sum of p_{cond} (long-range interactions) and p_{el} calculated according our model (short-range interactions) gives practically the result of Fixman's calculations, which took into account both types of interactions (dotted curve in Fig. 3). Thus, the main source of an experimentally observed increase in the DNA persistence length at low ionic strength is a change of the long-range electrostatic interactions, i.e., the electrostatic bending energy at very low ionic strength becomes non-additive with respect to contributions from individual nearest neighbors along the polyion axis. An increase in ionic strength leads to a rapid decrease of the long-range interactions (see Eq. (32)) and then the persistence length depends on salt concentration very slightly: this dependence can be approximated according to our model as $p_{el} \approx 6.61\ C^{-0.12}$ nm. At the ionic strength above 10 mM only the short-range interactions contribute into the electrostatic bending energy of DNA. Since our model is more simple than those of Fixman and Le Bret, it can be easily applied to estimate the electrostatic energy of uniform DNA bending in protein–DNA complexes at moderate ionic strength.

5. Electrostatic contribution to DNA bending in complexes with proteins

It has been suggested early that an asymmetric neutralization of charges on the DNA surface may play an important role as driving force for DNA bending (particularly, in the nucleosome) [30]. This hypothesis was confirmed by the simple analysis based on the condensation theory [31] and by the experimental studies of a chemically modified DNA [32,33]. As discussed above, the electrostatic contribution into DNA bending rigidity is very low (at moderate salt concentrations). It can be expected, however, that bending-induced decrease in the surface charge density on the opposite to protein side of DNA (see Fig. 2) would be accompanied by a release of a fraction of counterions into the bulk solution and then an increase in the entropy of the system [34]. Our model allows us to estimate, on the basis of a non-linear PB equation, the electrostatic free energy of DNA bending in the case of an asymmetric neutralization of a fraction θ of DNA surface by a protein in the direction of the curvature.

The dependencies of the free energy on θ at given values of the ionic strength are presented in Fig. 4. One can see that the electrostatic contribution to the bending free energy, which is small and positive (bending is unfavorable) for the naked DNA ($\theta = 0$), becomes more significant and negative with an increase in the degree of the asymmetric neutralization of DNA charge, i.e., the bending of DNA in

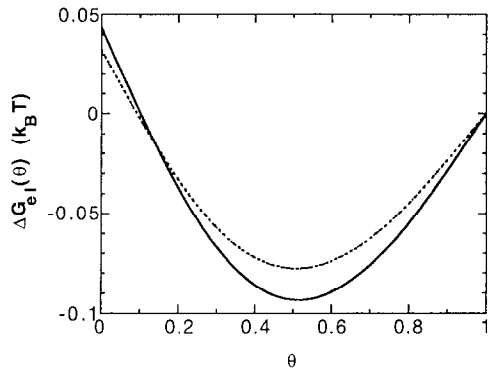

Fig. 4. The dependencies of the DNA bending free energy (per one phosphate, Eq. (22)) on the degree of the asymmetric neutralization θ at the molar concentrations of 1:1 salt 0.01 (smooth curve) and 0.1 (dashed curve) for the curvature radius $R = 5$ nm.

the case of asymmetric neutralization is a favorable process with respect to electrostatic interactions. The effect has a maximum at $\theta = 0.5$, i.e., when the side of the polyion with increased charge density is totally neutralized. Then, the increase in θ leads to the increase in the free energy which necessarily tends to zero at $\theta = 1$. The salt-dependence of the electrostatic free energy of asymmetrically neutralized DNA is shown in Fig. 5. For a comparison, the constant non-electrostatic contribution to the bending energy (per one phosphate at $p_0 = 50$ nm and $R = 5$ nm, see Eq. (24)) is $+0.17\ k_BT$, i.e., a significant part of this value is balanced by the negative electrostatic contribution in DNA-protein complexes at moderate ionic strength.

The electrostatic contribution clearly depends on θ, curvature radius R and ionic strength C. There is a value of the curvature radius R_m that corresponds to a maximum gain in the electrostatic bending free energy at given θ and C. If the total free energy of DNA bending in a protein–DNA complex is

$$\Delta G_{bend} = \Delta G_{el}(\theta) + bp_0/2R^2 \qquad (33)$$

then, after substitution of Eq. (22) and appropriate differentiation, we obtain:

$$R_m = -\frac{bp_0 + 2\pi I_{20}(1-\theta) + I_{22}\sin(2\pi(1-\theta))}{kI_{11}\sin(\pi(1-\theta))} \qquad (34)$$

The dependencies of R_m upon the ionic strength at given values of θ are shown in Fig. 6. It is interesting that, in the region of physiological salt concentrations (ca. 100 mM), $R_m \approx 4$–5 nm, which is exactly corresponds to the observed DNA curvature in, for example, nucleosome particle [1], DNA–gyrase complex [35] and complexes of DNA with a conservative HMG-box of a series of DNA–binding proteins [36]. The same curvature has been detected after asymmetric removal of phosphate charges in chemically modified DNA [32].

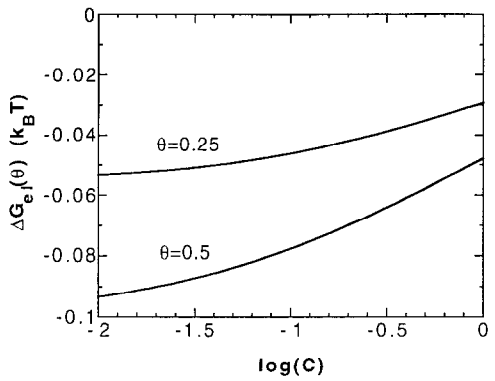

Fig. 5. The dependencies of the DNA bending free energy (per one phosphate, Eq. (22)) on the molar concentration of 1:1 salt for the curvature radius $R = 5$ nm and two designated values of the degree of the asymmetric neutralization θ.

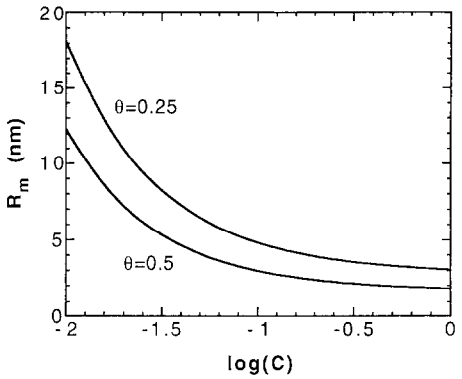

Fig. 6. The curvature radius that corresponds to a maximum gain in the electrostatic bending free energy (for the given degrees of the lateral neutralization θ, if the non-electrostatic contribution to the persistence length $p_0 = 50$ nm) as a function of molar concentrations of 1:1 salt (Eq. (27)).

6. Implication to the nucleosome

In the nucleosome, the elementary unit of eukaryotic chromatin structure, DNA (about 145 base pairs) wraps around an octamer of the histone proteins with an average curvature radius 4.3 nm [1]. The structure is stabilized by the electrostatic interactions between histones and phosphate residues and these interactions are essentially asymmetric: the outer surface of the nucleosome DNA is accessible to different agents (see Ref. [2] for a review). The degree of the phosphate charge neutralization is unknown exactly, but it can be approximately estimated as 20–25% due to interactions with the globular parts of the histones [1]. The positively charged unfolded histone tails additionally increase the degree of neutralization till to approximately 50% at low and moderate ionic strength. These tails dissociate from DNA within the

range of 0.2–0.6 M NaCl, when the nucleosome structure retains its stability [37].

We have employed our model (Eq. (22) and numerical results) to estimate the electrostatic contribution to the free energy of DNA deformation in the nucleosome. The dependencies of this contribution upon the ionic strength (per 290 phosphates, for $R = 4.3$ nm, and $\theta = 0.25$ and 0.5) are presented in Fig. 7. The constant non-electrostatic contribution to the energy of the nucleosome DNA deformation is (according to Eq. (24) with $p_0 = 50$ nm) + $66.7k_BT$. The electrostatic contribution (see Fig. 7) changes between 10 and 100 mM salt from $-16.5k_BT$ to $-14.5\ k_BT$ for $\theta = 0.25$ and from $-30.3k_BT$ to $-25.3k_BT$ for $\theta = 0.5$. Thus, about 20–40% of non-electrostatic contribution is balanced by the electrostatic bending free energy at moderate ionic strength, i.e., asymmetric neutralization significantly stabilizes the nucleosome structure.

Fig. 7 presents also the results of the same calculations, but for the hypothetical case of the symmetric (uniform with respect to φ angle) neutralization of the surface charge. In this case we consider the polyion with decreased with respect to DNA axial charge density, i.e., Eq. (23) is used, where I_{20} is obtained numerically for $\xi = \xi_{DNA}(1 - \theta)$, $\xi_{DNA} = 4.2$. The dramatic difference between uniform and asymmetric neutralization is observed. We might envisage, on the basis of this phenomenon, a simple mechanism of functionally important destabilization of the nucleosome structure in transcriptionally active regions of chromatin. One can see from Fig. 7 that the binding of positively charged ligand to the outer surface of the nucleosome DNA would be sufficient to decrease considerably the stability of the bent state of the nucleosome DNA.

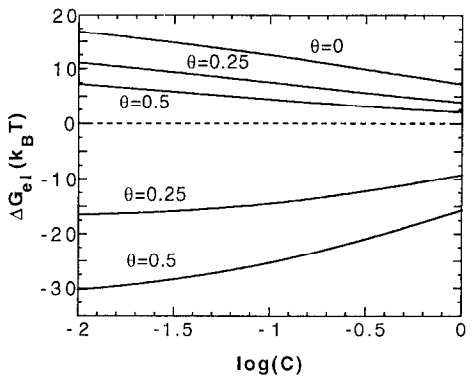

Fig. 7. The electrostatic contribution to the free energy of DNA bending in the nucleosome (per 290 phosphates, the curvature radius is 4.3 nm) as a function of molar concentrations of 1:1 salt for designated values of the degree of neutralization. Three upper curves (within the positive range of the energy) are calculated for the uniform (with respect to angle φ) neutralization, two lower curves (within the negative range of the energy) are for the asymmetric neutralization.

7. Conclusions

The considerations of polyelectrolyte properties of DNA on the basis of condensation hypothesis [20], PB equation [25,38,39] and more detailed calculations [39–42] indicate that the local concentration of counterions near the polyion surface is very high (> 1 M) even at low bulk salt concentrations and, consequently, the charge on phosphate residues is essentially screened. Appendix A illustrates (see Ref. [27] for details) that the major contribution to the electrostatic free energy is the mixing entropy of the mobile ions, i.e., the decrease in entropy due to assembling the ion atmosphere around the polyion. If DNA molecule bends, a rearrangement of the ion atmosphere occurs and, respectively, the free energy changes. Our analysis of the PB equation implies that these changes consist of two terms that can be considered separately. First, the short-range (with respect to distance along the polyion axis) electrostatic interactions, which depend on the changes in the polyion surface charge density under deformation. Second, the long-range electrostatic interactions, which depend on the bending-induced changes of distances between each two points along the axis.

In the present work, we have restricted our analysis of the electrostatic contribution to the DNA persistence length to the short-range electrostatic interactions. The numerical solution of the corresponding PB equation allows us to obtain the lower limit for the electrostatic persistence length of DNA. The contribution of the short-range electrostatic interactions to the bending free energy is positive (unfavorable), not so significant, and depends only slightly on the ionic strength. In the case of random bending fluctuations of the polymer in solution, the long-range electrostatic interactions cannot be easily

taken into account. These interactions have been included into consideration by Fixman [22] and Le Bret [23], but for a uniformly bent polyion. Hence, the results of Fixman–Le Bret give the upper limit for the electrostatic persistence length of DNA. Comparison between the theories and experiment [9–12], indicates that the actual behavior of the DNA persistence length lies between two theoretical limits and that the experimentally observed increase in the DNA persistence length at low ionic strength mainly depends on the long-range electrostatic interactions. This conclusion is in an agreement with the earlier calculations of the electrostatic persistence length, which took into account, in Debye–Hückel approximation, the long-range interactions only [17–19]. According to comparison of our results with the data of Fixman [22] and Le Bret [23], the long-range electrostatic interactions in the uniformly bent polyion are negligible at the ionic strength above 10 mM (for a 1:1 salt), and, as it is ensued from the experimental results [9], these interactions lead to an essential increase in the DNA persistence length below 1 mM of 1:1 salt.

The mixing entropy of mobile ions is the dominant contribution into the total electrostatic free energy (see Appendix A). The small electrostatic contribution to the persistence length (in comparison with its total value) and slight dependence of the persistence length upon the ionic strength implies that the bending-induced rearrangement of mobile ion atmosphere does not lead to a significant change of the electrostatic free energy. The results obtained by Fixman [26] and Fenley et al. [24] show that there is essentially no extra accumulation of counterions due to DNA bending. That is, qualitatively, an additional accumulation of mobile ions near the regions of polyion surface with increased charge density is approximately balanced by a losing of them on the opposite side of the polyion where its surface charge density decreases. Our analysis indicates that the release of counterions from the side with decreased charge density becomes uncompensated in the case of asymmetric neutralization of the DNA charge by a protein. Therefore, the electrostatic bending energy gives a significant negative (favorite) contribution to the total bending energy of DNA, or, in other words, DNA bending in the complexes with proteins gives an advantage in the electrostatic free energy. This theoretical conclusion provides an additional insight into the mechanisms of the DNA–protein interactions.

For example, implication of our model to the nucleosome structure, where DNA charge is asymmetrically neutralized by the histone proteins, shows that the negative electrostatic contribution is about 20–40% (in the absolute values) of the positive non-electrostatic free energy of DNA bending in the nucleosome. So, the contribution from the electrostatic bending free energy significantly stabilizes the nucleosome structure. On the other hand, the binding of a positively charged ligand to the outer surface of the nucleosome DNA might lead to a more uniform charge neutralization and then, as it is indicated by our calculations, to a considerable decrease in stability of the bent state of the nucleosome DNA. This effect may be one of the mechanisms of functionally important destabilization of the nucleosome structure in transcriptionally active regions of chromatin [43].

Appendix A. Contributions to the total electrostatic free energy of DNA

The electrostatic free energy of the polyion can be defined not only as the charging integral (Eq. (12)), but also can be equivalently calculated by the integration of functions of the electrostatic potential over the volume of the ion atmosphere around the polyion. According to the comprehensive analysis of the PB equation by Sharp and Honig [27], the total electrostatic free energy of DNA modeled by the straight uniformly charged cylinder (in k_BT units per one elementary charge of the polyion) can be written as:

$$G_{el} = (4\xi)^{-1} \int_a^{\infty} \left[(df/dr)^2 + 2k^2 f \sinh(f) - 2k^2(\cosh(f) - 1) \right] r\,dr \qquad (1A)$$

where $f \equiv f_0$ in our definitions. Three terms under the integral in Eq. (1A) have a clear physical meaning [27]. The first term is the energy of the electrostatic field of the polyion. This term would be the single contribution to the energy in vacuo, but in solution the electrostatic field is considerably reduced by the mobile ions (even in the absence of added salt [25,38]). The second term relates to the

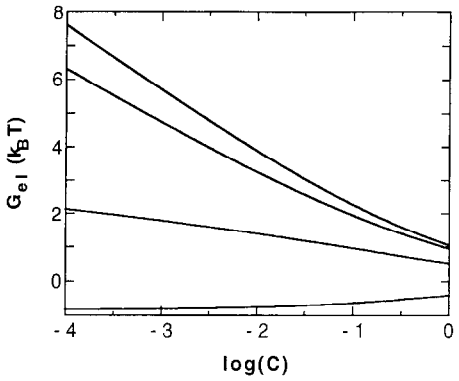

Fig. 8. The contributions to the electrostatic free energy of DNA, modeled by straight uniformly charged cylinder, as functions of molar concentrations of 1:1 salt. Curves represent (from top to bottom): the total free energy, the contribution from the mobile ion mixing entropy, the energy of the electrostatic field, and the osmotic pressure contribution.

entropy change of the ion atmosphere with respect to the bulk solution. The third term is the contribution from the osmotic pressure of the ion atmosphere. All terms can be calculated after numerical solution of the PB equation for a straight cylinder (Eq. (5)). The results of calculations for the different ionic strength are presented in Fig. 8. The values of the total free energy, as calculated according to Eq. (1A), practically coincide (± 0.001) with the values obtained on the basis of Eq. (12). One can see from Fig. 8 that the major contribution to the electrostatic free energy is the second term in Eq. (1A), which relates to the mixing entropy of mobile ions. This fact can be considered as an additional physical foundation of the condensation theory in the PB equation.

References

[1] T.J. Richmond, J.T. Finch, B. Rushton, D. Rhodes, A. Klug, Nature (London) 311 (1984) 532.
[2] A. Wolffe, Chromatin. Structure and function, Academic Press, London, 1992.
[3] A.A. Travers, Annu. Rev. Biochem. 58 (1989) 427.
[4] A.V. Sivolob, S.N. Khrapunov, J. Mol. Biol. 247 (1995) 918.
[5] T.K. Kerpola, T. Curran, Science 254 (1991) 1210.
[6] S.C. Schultz, G.C. Shields, T.A. Steitz, Science 253 (1991) 1001.
[7] Y. Kim, J.H. Greger, S. Hahn, P.B. Sigler, Nature (London) 356 (1993) 512.
[8] L.C. Lutter, H.R. Halvorson, C.R. Calladine, J. Mol. Biol. 261 (1996) 620.
[9] P.J. Hagerman, Biopolymers 20 (1980) 1503.
[10] Z. Kam, N. Borochov, H. Eisenberg, Biopolymers 20 (1981) 2671.
[11] K.L. Cairney, R.E. Harrington, Biopolymers 21 (1982) 923.
[12] W.H. Taylor, P.J. Hagerman, J. Mol. Biol. 212 (1990) 363.
[13] D. Pörschke, Biophys. Chem. 40 (1991) 169.
[14] J.M. Shurr, K.S. Schmitz, Annu. Rev. Phys. Chem. 37 (1986) 271.
[15] P.J. Hagerman, Annu. Rev. Biophys. Biophys. Chem. 17 (1988) 265.
[16] V.A. Bloomfield, D.M. Crothers, I. Tinoco, Physical Chemistry of Nucleic Acids, Harper and Row, New York, 1974.
[17] T. Odijk, J. Polym. Sci. Polym. Phys. Ed. 15 (1977) 477.
[18] J. Skolnick, M. Fixman, Macromolecules 10 (1977) 944.
[19] T. Odijk, A.C. Houwaart, J. Polym. Sci. Polym. Phys. Ed. 16 (1978) 627.
[20] G.S. Manning, Q. Rev. Biophys. 11 (1978) 179.
[21] G.S. Manning, Biopolymers 20 (1981) 1751.
[22] M. Fixman, J. Chem. Phys. 76 (1982) 6346.
[23] M. Le Bret, J. Chem. Phys. 76 (1982) 6243.
[24] M.O. Fenley, G.S. Manning, W.K. Olson, J. Phys. Chem. 96 (1992) 3963.
[25] C.F. Anderson, M.T. Record, Annu. Rev. Phys. Chem. 33 (1982) 191.
[26] M. Fixman, J. Chem. Phys. 92 (1990) 6283.
[27] K.A. Sharp, B. Honig, J. Phys. Chem. 94 (1990) 7684.
[28] P.J. Hagerman, Biopolymers 22 (1983) 811.
[29] K.R. Hagerman, P.J. Hagerman, J. Mol. Biol. 260 (1996) 207.
[30] A.D. Mirzabekov, A. Rich, Proc. Natl. Acad. Sci. USA 76 (1979) 1118.
[31] G.S. Manning, K.K. Ebralidze, A.D. Mirzabekov, A. Rich, J. Biomol. Struct. Dynam. 6 (1989) 877.
[32] J.K. Strauss, L.J. Maher III, Science 266 (1994) 1829.
[33] J.K. Strauss, C. Roberts, M.G. Nelson, C. Switzer, L.J. Maher III, Proc. Natl. Acad. Sci. USA 93 (1996) 9515.
[34] D.M. Crothers, Science 266 (1994) 1819.
[35] D.C. Rau, M. Gellert, F. Thoma, A. Maxwell, J. Mol. Biol. 193 (1987) 555.
[36] C.M. Read, P.D. Cary, N.S. Preston, N. Lnenicek-Allen, C. Crane-Robinson, EMBO J. 13 (1994) 5639.
[37] I.O. Walker, Biochemistry 23 (1984) 5622.
[38] M. Le Bret, B.H. Zimm, Biopolymers 23 (1984) 287.
[39] M.D. Paulsen, C.F. Anderson, M.T. Record, Biopolymers 27 (1988) 1249.
[40] M. Le Bret, B.H. Zimm, Biopolymers 23 (1984) 271.
[41] P. Mills, C.F. Anderson, M.T. Record, J. Phys. Chem. 89 (1985) 3984.
[42] B. Jayaram, K.A. Sharp, B. Honig, Biopolymers 28 (1989) 975.
[43] G. Felsenfeld, Cell 86 (1996) 13.